

# 200-W Tm:YLF INNOSLAB Laser

A. Meissner<sup>\*a</sup>, J. Li<sup>b</sup>, I. Lopez-Perez<sup>a</sup>, S. Yang<sup>b</sup>, M. Hoefler<sup>a</sup>, D. Hoffmann<sup>a</sup>,

<sup>a</sup>Fraunhofer Institute for Laser Technology, Steinbachstr. 15, 52074 Aachen, Germany;

<sup>b</sup>School of Optoelectronics, Beijing Institute of Technology, Beijing 100081, China

## ABSTRACT

A Tm:YLF laser in INNOSLAB design is reported. It produces 200 W of output power at an optical efficiency of 24 % and a slope efficiency of 27 % with respect to incident pump power. The laser crystal is partially end-pumped in a top-hat line focus with a width of 12 mm and a height of about 1 mm. It is placed in a stable, spherical laser resonator, which results in a highly elliptical output beam. The beam is near diffraction limit and Gaussian in shape in one axis and contains very high order transversal modes and is Top-Hat-like in shape in the other axis. The beam shape is ideal for pumping a Ho:YLF laser crystal in INNOSLAB design for a pulsed amplifier.

**Keywords:** High-Power, 2 micron, Tm:YLF, Slab laser, Top-Hat

## 1. INTRODUCTION

There has been increasing interest in lasers emitting around 2  $\mu\text{m}$  because they have a variety of applications: The strong water absorption enables medical applications like tissue ablation. [1] They can also be used for remote sensing of atmospheric trace gases like CO<sub>2</sub> and defense applications like range finding and missile counter measures. [2] [3] Laser emission around 2  $\mu\text{m}$  provides an efficient pump source for OPO and OPA-systems in the mid infrared spectrum. Not finally, many materials which are transparent in the VIS region and are thus commonly processed with UV lasers can be structured with laser radiation in the 2  $\mu\text{m}$ -regime.

Both, Thulium (Tm) and Holmium (Ho) as dopants in solid-state laser materials have prominent transitions in the 2  $\mu\text{m}$  spectral region. Due to an inter-ionic down conversion process at doping levels of several percent, Tm can be efficiently pumped with well-established high-brightness laser diodes at about 800 nm. An appropriate choice of the doping level can lead to a quantum efficiency of close to 2, which almost totally compensates the high quantum defect of about 60 %. However, the emission cross section of the 2  $\mu\text{m}$  transition in the Tm-ion is very low (in the range of  $1 - 5 \cdot 10^{-21} \text{ cm}^2$ ) [4], which is problematic particularly in energy storage operation because saturation fluence then exceeds usual damage limits of optical coatings. In cw mode of operation, this problem is mitigated by the long storage time of about 5 – 10 ms, yielding moderate saturation intensities. Holmium, in turn, has about 5 times larger emission cross sections and is thus a feasible dopant for a laser in energy storage mode, but it cannot be pumped with 800-nm diodes. Fortunately, radiation emitted from Tm-lasers can efficiently pump Ho-crystals. It is therefore a well-established approach for a slowly repeating pulsed laser to use a cw Tm-laser for pumping the pulsed Ho-laser.[5]

The ILT-proprietary INNOSLAB laser concept provides superior heat management capabilities which enables generation of high-power and high-energy laser emission in diffraction limited beams. The laser crystal geometry matches the typical beam shapes of diode laser bar stacks, which greatly simplifies the required pump beam shaping and thus increases its transfer efficiency.[6][7][8][9]

## 2. LASER DESIGN

The ILT-proprietary INNOSLAB laser concept was used, which is described in detail in [6], but shall be briefly outlined in the following. It consists of a slab-shaped laser crystal which typically is about 1 to 4 mm thick, 10 to 40 mm wide and 10 to 30 mm long, thus providing two very large surfaces (top and bottom of the slab) for effective heat dissipation. These two surfaces are thermally contacted to heat-sinks. Other than in conventional slab laser concepts, the INNOSLAB laser crystal is partially end-pumped with stacked diode-laser bars. The beam shaping of the diode-laser bars generates a pump line in the laser crystal which is nearly top-hat-like in slow axis (x-axis in the following) and matches the slab crystal width in its size. This way, the slab crystal in this axis is homogeneously pumped. In fast axis (y-axis in the following), however, all bars are focused into the laser crystal and provide a Gaussian pump light distribution which is

smaller than the slab crystal's height. With proper choice of the degrees of freedom in pump light beam shaping and crystal geometry, heat is extracted from the laser crystal very efficiently and only in fast axis exists an unaberrated thermal lens while in slow axis no thermal lensing occurs.

Mostly, this INNOSLAB laser crystal setup is combined with a stable-unstable hybrid resonator in order to provide spherical, diffraction limited output beams. [6][7][8] Here, however, the application of the described laser was pumping a Ho-crystal in INNOSLAB geometry. Consequently, the shape of the laser beam emitted by the described laser was required to be similar to that of typical diode-laser bar stacks: highly elliptical with a diffraction-limited near Gaussian shape in one direction and a top-hat like, very high-order mode-structure in the other direction. It is obvious, that this can be achieved from the described laser crystal and pump geometry by putting it in an appropriate purely spherical laser resonator, which was demonstrated before [10] and done here, as well.

## 2.1 Pumping Scheme

The laser crystal was an YLF host with 2.5 at-% doping of Thulium. It had a height of 2 mm (in the direction of the crystal's c-axis), a width of 12 mm and a length of 20 mm. As a pump source, two fast-axis collimated 6-bar diode-laser stacks with an emission wavelength of about 792 nm were used. The maximal optical output power of each 6-bar stack was 430 W. Beam shaping of these stacks was performed with ILT's standard pump optics, which was developed and used for Nd-doped laser crystals. It has an effective focal length in y-direction of 40 mm.

With a simulation tool, which was developed at ILT before, the absorbed pump power distribution in the (y,z)-plane of the laser crystal was predicted. The tool makes use of the ABCD-Matrix formalism for propagating each individual laser diode bar of the stack through definable pump optics into the laser medium. In the laser medium, the fast-axis distribution of the pump light from each individual stack is approximated by a Gaussian distribution with beam radius, divergence angle, steering angle and beam center position as computed by the ABCD-Matrix formalism. With this distribution of incident pump light, the absorption of the pump beam with the simulated shape is then computed. Input parameters for the simulation tool are the fast axis diode bar divergence angle, the pitch between individual bars of the stacks, the beam radius of the light emitted from an individual bar, the number of bars per stack and the geometry and the pump light absorption coefficient of the laser crystal. In the presented case, the used values for the parameters were  $0.5^\circ$  of fast axis divergence angle of diode laser bar (behind FAC), 1.75 mm pitch between bars, 500  $\mu\text{m}$  beam radius for individual bar (behind FAC) and an absorption coefficient of  $0.12 \text{ mm}^{-1}$ .

The result of this calculation is shown on the left hand side in Figure 1. It can be seen, that the pump light is absorbed in very confined regions while other regions in the the crystal center remain almost unpumped and will thus exhibit strong reabsorption losses for the laser wavelength in the quasi-three-level system of Tm. This pump optics is thus not feasible for the present Tm:YLF crystal.

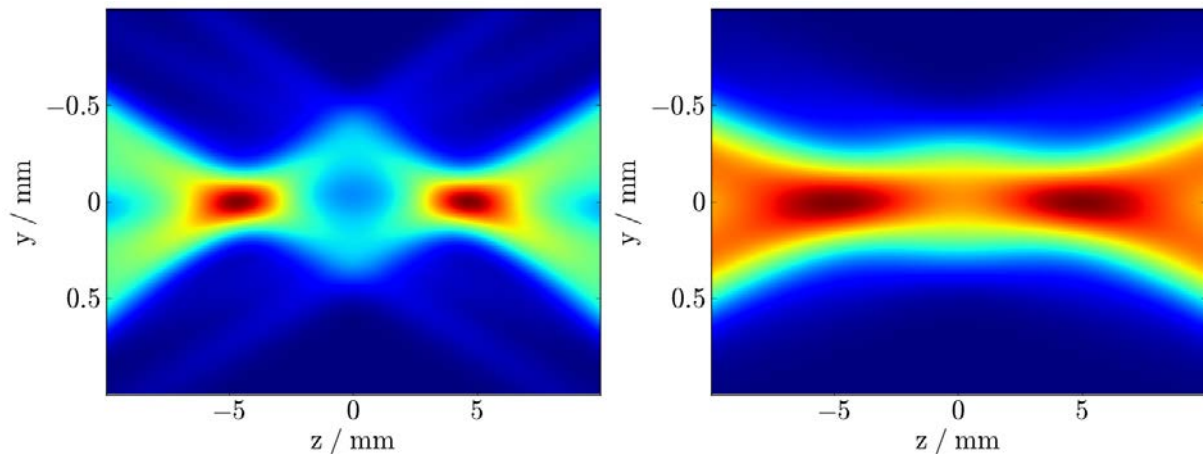


Figure 1. left: Calculated absorbed pump power distributon in the laser crystal in the (y,z)-plane with ILT's standard pump optics for Nd-doped crystals. Obviously, this pump optics is not appropriate for the present Tm:YLF-crystal. Right: The same calculation for a modified pump optics which has an additional diverging cylindrical lens in y-axis behind ILT's standard pump optics, providing an effective focal length of 60 mm.

Therefore, a defocusing cylindrical lens with a focal length of -100 mm was added in y-axis. It was located in the principal plane of the standard pump optics. This way, an effective focal length of the modified pump optics of 60 mm was established. The calculation of the absorbed pump power distribution is shown on the right hand side in Figure 1. With this pump optics, the absorbed pump light is distributed more homogeneously over the crystal's z-axis. Therefore, reabsorption losses are expected to be less pronounced.

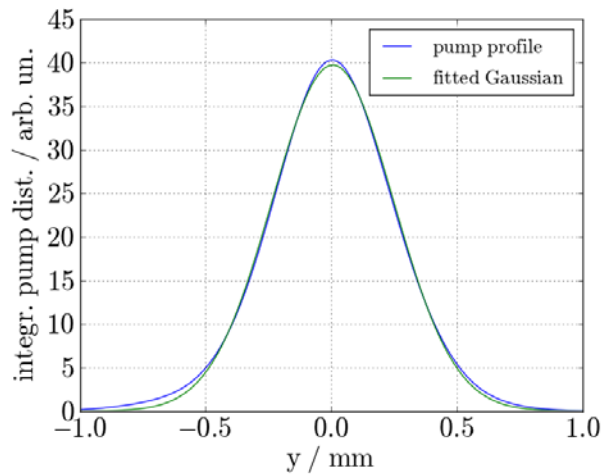


Figure 2. Effective pump light distribution along y-axis, which was calculated from Figure 1, right by integration over the z-axis. The 4-sigma width of the fitted Gaussian, which is also shown in the plot, was 970  $\mu\text{m}$ .

The absorbed pump power distribution as shown on the right hand side in Figure 1 was then integrated over the z-axis in order to obtain an effective pump light distribution along the y-axis. From this, an effective size in y-direction of the pumped volume could be computed by fitting a Gaussian to the effective pump light distribution. The integrated pump light distribution and the fitted Gaussian are shown in Figure 2. The 4-sigma width of the fitted Gaussian is 970  $\mu\text{m}$ .

## 2.2 Laser Resonator

A spherical plano-concave laser resonator was used. A sketch of the setup together with a definition of the symbols for relevant resonator parameters is shown in Figure 3.

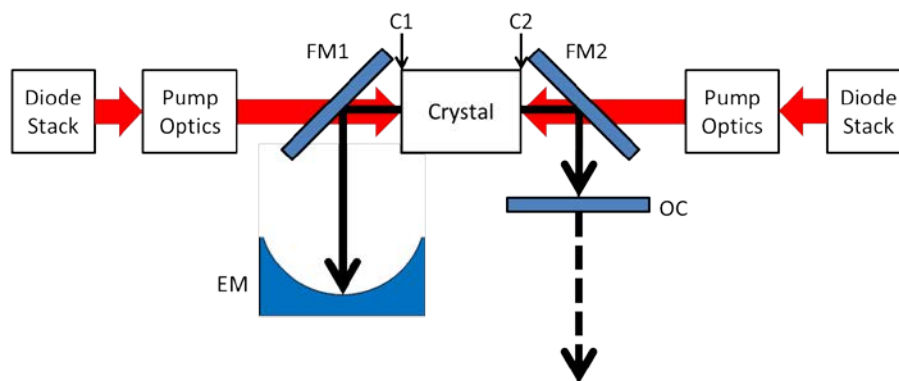


Figure 3. Schematic sketch of the laser oscillator setup. C1 and C2 mark the two optical faces of the laser crystal, FM1 and FM2 are dichroic folding mirrors, which are anti-reflective for pump light and highly reflective for the laser light, EM denotes the end mirror and OC the output coupler.

A plane output coupler provided a defined location of the beam waist where the beam exits the laser resonator. The concave end mirror was used to compensate the negative thermal lens of YLF along the  $\pi$ -polarization. The well-known inverse proportionality of the focal length of the thermal lens to the absorbed pump power is shown Figure 4. In order to reduce the susceptibility of the laser resonator mode to variations for the thermal lens, the laser crystal was placed as

close as possible to the plane output coupler, i.e. the distance between the laser crystal and the output coupler was 55 mm. Also, from Figure 4 it can be seen that for expected 700 W of absorbed pump power a thermal lens with  $f_{\text{thermal}}$  of about -150 mm can be expected.

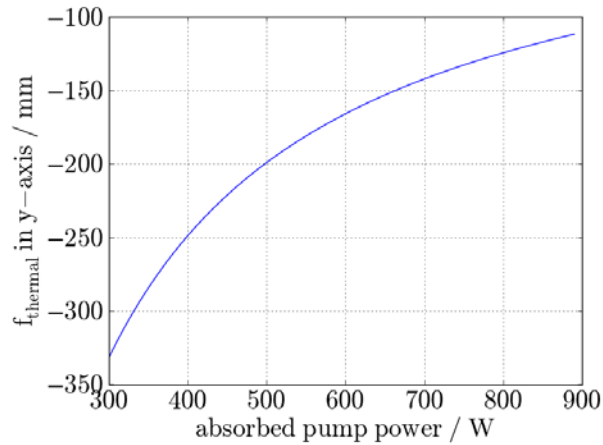


Figure 4. Focal length of the thermal lens in y-axis as a function of absorbed pump power for the given laser crystal and pump geometry. At expected absorbed pump power of about 700W the focal length is -150 mm.

A concave end mirror with a radius of curvature of 200 mm was used. The distance between the end mirror and the laser crystal was used for optimizing the overlap between the laser mode and the pumped volume in y-axis. Figure 5 shows the mode radius of the resonator's eigenmode in the center of the laser crystal as a function of the distance between the laser crystal and the end mirror. Additionally, the resonator's stability parameter  $g_1g_2$  is plotted. For this computation,  $f_{\text{thermal}} = -150$  mm and a distance between the laser crystal and the plane output coupler of 55 mm were assumed.

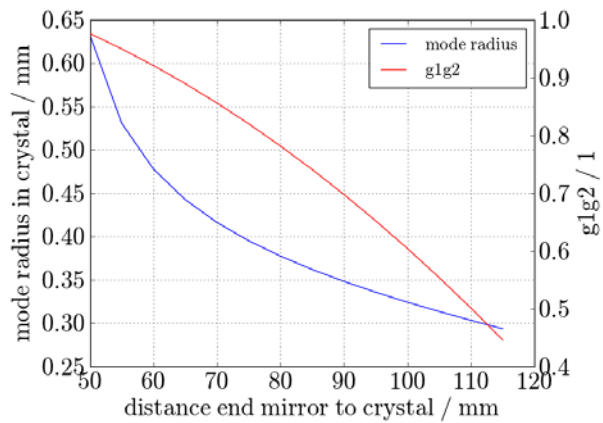


Figure 5. Mode radius of the resonator's eigenmode as a function of the distance from the end mirror to the laser crystal is plotted. The focal length of the thermal lens is assumed to be -150 mm, the length of the laser crystal is 20 mm and the distance between the laser crystal and the end mirror is set to 55 mm in this computation.

At a distance of about 60 mm, the mode radius in the crystal equals the height of the pumped volume in y-axis (c.f. Figure 2). However, experiments showed that a distance of 85 mm provides the highest output power where the mode radius is only about 360  $\mu\text{m}$ . This difference can be attributed to the reabsorption losses in unpumped regions: As can be seen from the right hand side of Figure 1, absorbed pump power distribution is not uniform along the z-axis. There are, in particular, two positions on the z-axis, namely at about +5 mm and -5 mm of the scale from Figure 1, where the absorbed pump power has the narrowest distribution along the y-axis. In Figure 6, the Gaussian laser mode with a mode radius of 360  $\mu\text{m}$  together with the absorbed pump power distribution along the y-axis at  $z = +5$  mm is depicted. The curves coincide and increasing the mode radius would increase reabsorption losses in the Gaussian tail of the mode.

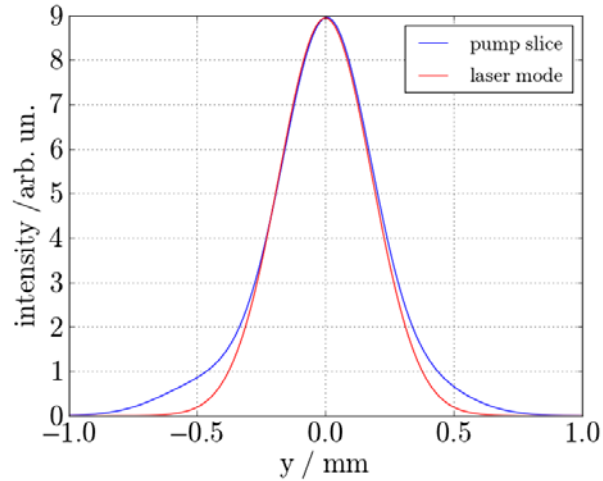


Figure 6. The computed absorbed pump power distribution at a position of  $z = 5$  mm inside the laser crystal is depicted in blue together with a Gaussian laser mode distribution with a mode radius of  $360 \mu\text{m}$  in red.

In Figure 7, the eigenmode of the used laser resonator with the distance from the end mirror to the laser crystal of 85 mm is shown. The location of the laser crystal is marked in blue. As described above, the mode radius in the laser crystal is  $360 \mu\text{m}$ . Please note that the  $z$ -axis is given in terms of optical path, so that the laser crystal is shorter in this plot by a factor of the refractive index of YLF than its geometrical length of 20 mm. The reflectivity of the output coupler was 80 %, which yielded the highest output power.

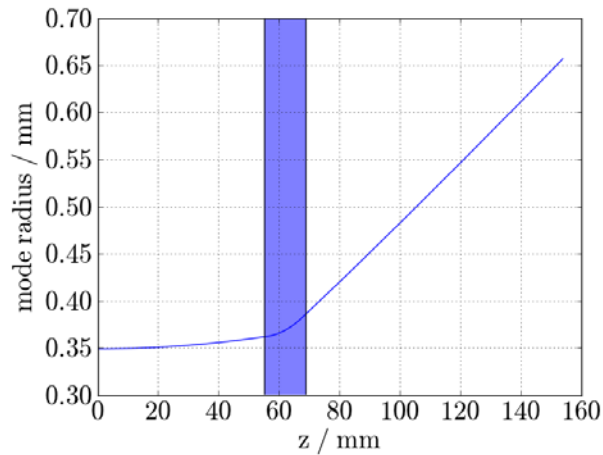


Figure 7. Calculated laser resonator eigenmode. The blue region marks the position of the laser crystal.

### 3. EXPERIMENTAL RESULTS

A maximal laser output power of 200 W was achieved at incident pump power of 850 W, corresponding to an optical efficiency of about 24 %. The input-output characteristic is shown in Figure 8. The slope efficiency was measured to be about 27 % and the laser threshold was reached at a pump power of 200 W. No thermal roll-over was observed. Also, the laser crystal did not show thermal fracture in any of the experiments, so that output power is limited by available pump power only. However, the available water cooling capacity was limited to about 300 W of heat. Therefore, at higher pump power the laser crystal heated up, so that high pump power could only be used for short periods of time.

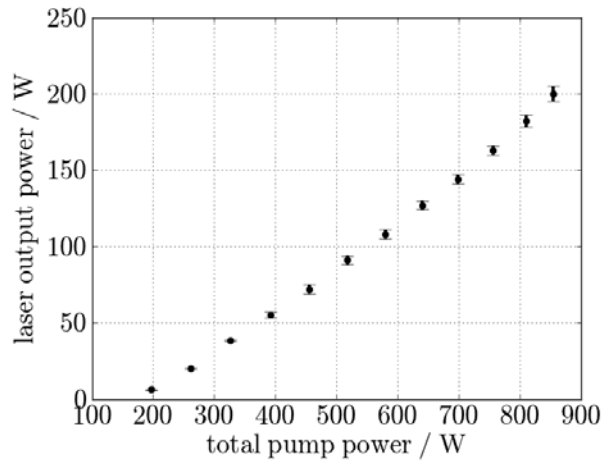


Figure 8. Measured laser output power as a function of the total irradiated pump power. Output power is limited by pump power. The optical efficiency is 24 %, the slope efficiency is 27 % and the laser threshold pump power is 200 W.

The emission wavelength and polarization state were not stable when the full pump power of 850 W was used. A mixture of  $\sigma$ - and  $\pi$ -polarization and the corresponding emission wavelengths of 1908 nm and 1888 nm, respectively, with unstable power fractions was observed. In order to select a single polarization and emission wavelength a Brewster plate was inserted in the laser resonator. Then, 160 W of output power could be measured at full pump power. Also, whenever a single polarization was selected the coating of the end mirror was damaged at moderate intracavity intensities of about 5 to 10 kW/cm<sup>2</sup>, which also explains the much lower output power with the Brewster plate.

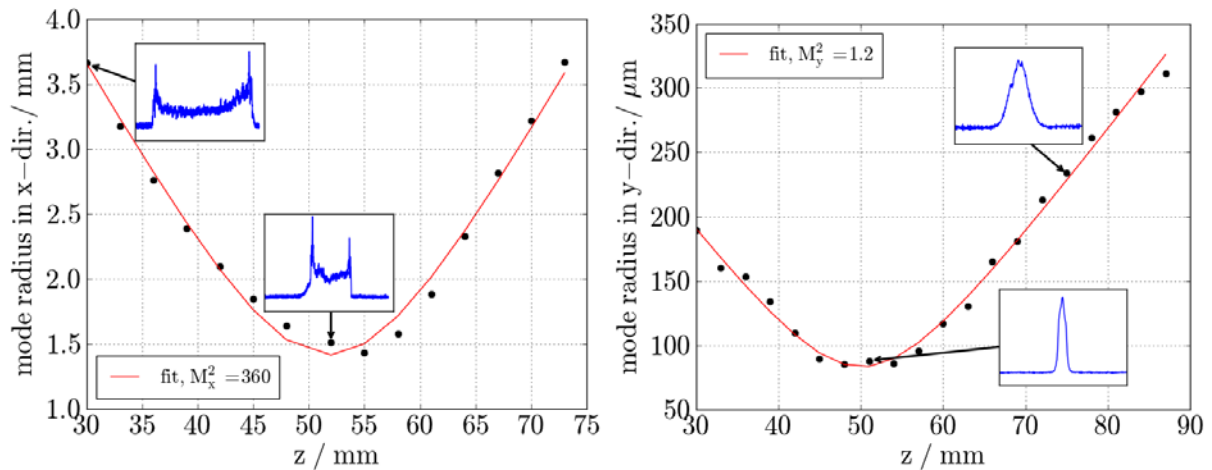


Figure 9. Measured beam caustics in x- and y-directions with fitted caustic curves. The inserts show the integrated beam shapes at the positions marked with the arrow.

Beam propagation parameters and beam profiles were measured at 50 W of laser output power, which was the maximal output power that could be established over a long period of time due to the insufficient cooling capacity. Beam profiles were measured with a slit-based beam profiler which measures integrated beam profiles along one axis. The measured caustics (1/e<sup>2</sup>-method) with fits of the two directions are given in Figure 9. The best fit beam propagation parameters were  $M_x^2 \approx 360$  and  $M_y^2 \approx 1.2$ .

#### 4. CONCLUSION

An INNOSLAB laser oscillator with Tm:YLF as laser crystal was reported. A maximal output power of 200 W was observed from an incident pump power of 850 W. The optical efficiency was measured to be 24 % at a slope efficiency of 27 % and a laser threshold pump power of 200 W. In y-direction the laser beam was diffraction limited with a

Gaussian shape while in x-direction the laser operated in very high order mode and exhibited a Top-Hat-like beam profile. Laser output power was limited by available pump power. It is expected that efficiency will be significantly increased when optimized pump optics will be used that have increased focal length of above 80 mm and thus distribute the absorbed pump power more uniformly over the z-axis in the crystal. Stable linearly polarized operation was prevented by damage of the high reflection coating of the end mirror, which is expected to be overcome when a high-power 2  $\mu\text{m}$  high reflection coating is used. In further work, this laser will be used for pumping a pulse amplifier in INNOSLAB design with Ho:YLF as laser crystal.

## REFERENCES

- [1] LISA Laser products GmbH, "Versatile Holmium laser for Urology, Spine, Arthroscopy and ENT" <http://www.lisalaser.de/Lisa/images/stories/PDF/Sphinx.pdf>
- [2] European Space Agency (ESA), "A-SCOPE – Advanced Space Carbon and Climate Observation of Planet Earth, Report For Assessment", ESA-SP1313/1 (2008), available at [http://esamultimedia.esa.int/docs/SP1313-1\\_ASCOPE.pdf](http://esamultimedia.esa.int/docs/SP1313-1_ASCOPE.pdf).
- [3] Ehret, G., Kiemle, C., Wirth, M., Amediek, A., Fix, A., Houweling, S., "Space-borne remote sensing of CO<sub>2</sub>, CH<sub>4</sub>, and N<sub>2</sub>O by integrated path differential absorption lidar: a sensitivity analysis", Applied Physics B 90, 593-608 (2008).
- [4] Eichhorn, M., "Quasi-three-level solid-state lasers in the near and mid infrared based on trivalent rare earth ions," Appl. Phys. B 93, 269-316 (2008).
- [5] Scholle, K., Lamrini, S., Koopmann, P., Fuhrberg, P., [Frontiers in Guided Wave Optics and Optoelectronics], edited by Bishnu Pal, ISBN 978-953-7619-82-4, InTech, 2010.
- [6] Du, K., Wu, N., Xu, J., Giesekus, J., Loosen, P., Poprawe, R., „Partially end-pumped Nd:YAG slab laser with a hybrid resonator,” Optics Letters, Vol. 23, No. 5 (1998).
- [7] Luttmann, J., Nicklaus, K., Morasch, V., Fu, S., Hofer, M., Traub, M., Hoffmann, D., Treichel, R., Wührer, C., Zeller, P., „Very high-efficiency, frequency-tripled, Nd:YAG MOPA for spaceborne lidar,” Proc. SPIE 6871, 687109 (2008)
- [8] Loehring, J., Meissner, A., Hoffmann, D., Fix, A., Ehret, G., Alpers, M., „Diode-pumped single-frequency-Nd:YGG-MOPA for water-vapor DIAL measurements: Design, setup and performance,” Appl. Phys. B 102, No. 4, 917-935 (2011)
- [9] Strauss, H. J., Preussler, D., Collet, O. J. P., Esser, M. J. D., Jacobs, C., Bollig, C., Koen, W., Nyangaza, K., „330 mJ, 2  $\mu\text{m}$ , Single Frequency, Ho:YLF Slab Amplifier,” Advanced Solid-State Photonics, ATuA4 (2011).
- [10] Schellhorn, M., Ngcobo, S., Bollig, C., „High-power diode-pumped Tm:YLF slab laser,” App. Phys. B: Lasers and Optics 94, 195-198 (2009).